Electronic Supplementary Material (ESI) for Chemical Communications


**Supporting Information**

# Hollow spherical mesoporous phosphosilicate nanoparticles as a delivery vehicle for an antibiotic drug

Swapan K. Das,[a] Manas K. Bhunia,[a] Debrup Chakraborty,[b] Anisur Rahaman Khuda-Bukhsh[b] and Asim Bhaumik*

[a]*Department of Materials Science, Indian Association for the Cultivation of Science, Jadavpur, Kolkata – 700 032, India*

[b]*Cytogenetics and Molecular Biology Laboratory, Department of Zoology, University of Kalyani, Kalyani-741235, India*

*Address for correspondence. E-mail: msab@iacs.res.in

## Table of contents

## ***Section S1: Materials and Methods:***

**Materials.** Triblock copolymer poly(ethylene glycol)-*block*-poly-(propylene glycol)-*block*-poly(ethylene glycol) (Pluronic F127, $M_{av}$ = 12600, $EO_{106}PO_{70}EO_{106}$) was used as the structure-directing agent, 1,2,4–trivinylcyclohexane (TVCH) and tetraethyl orthosilicate (TEOS) and tetracycline (used as antibiotic drug) were purchased from Sigma-Aldrich. Hydrochloric acid (HCl) and orthophosphoric acid ($H_3PO_4$) were obtained from Merck. $CaCl_2$. $6H_2O$, $MgCl_2$. $6H_2O$, anhydrous $ZnCl_2$ and $CuCl_2$. $6H_2O$ were obtained from Merck. All chemicals were used without further purification.

**Preparation of Hollow Sphere Mesoporous Phosphosilicate Nanoparticles (HSMPSNPs).** In a typical synthesis, amphiphilic tri-block copolymer pluronic F127 (1.0 g) was added to 30 mL2.36 (N) aqueous hydrochloric acid (HCl) under vigorous stirring and was allowed to stir until dissolution. After dissolving, 1.3 g 1,2,4-trivinylcyclohexane (TVCH) was added slowly into it and allowed to stir for overnight. Then it was aged for 24 h at room temperature. After one day, 2.08 g tetraethyl orthosilicate (TEOS) was added slowly to the micellar solution and allowed to stir for 30 minutes. Then 1.16 g orthophosphoric acid ($H_3PO_4$) taken in 4 mL water was added to that solution under vigorous stirring and total mixture was stirred again for overnight at ambient condition. After that the mixture was covered and aged for a week at room temperature. Then it was transferred into an autoclave, aged at 373 K for 48 h. The molar composition of the gel synthesis mixture was 1.0:0.1-1.0:0.008:0.8:5.6:139 TEOS:$H_3PO_4$:F127:TVCH:HCl:$H_2O$. The samples were abbreviated as HSMPSNPs-(R) where R denotes the $n_{Si}/n_P$ molar ratio. The resultant solid was filtered, washed with distilled water and dried at 373 K. Finally, the obtained solid samples were calcined by slowly increasing the

temperature to 773 K (1 K $min^{-1}$ ramping rate) followed by heating at 773 K for 5 h in the presence of air to obtain template-free hollow sphere mesoporous phosphosilicate nanoparticles. Four samples with different input $n_{Si}/n_P$ molar ratios of 1.0, 2.0, 4.0 and 10.0 have been synthesized and these are designated as HSMPSNPs-1, HSMPSNPs-2, HSMPSNPs-4 and HSMPSNPs-10, respectively.

**Preparation of Tetracycline Loaded Hollow Sphere Mesoporous Phosphosilicate Nanoparticles (HSMPSNPs).** 20 mg of tetracycline was dissolved in 40 mL dichloromethane in a round bottom flask. Then to this solution 200 mg HSMPSNPs powdered sample was dispersed and allowed to stir for 4 h at ambient temperature in the dark condition. Then the mixture was carefully filtered and washed several times with dichloromethane and absolute ethanol and repeated the same procedure for another two times. Lastly tetracycline loaded yellow powder was obtained. The loading of drug within the HSMPSNPs was confirmed by UV-vis diffuse reflectance spectroscopy (Shimadzu UV 2401PC).

**Study of Controlled Release of Drug Molecules.** 20 mL aqueous solutions of different bio relevant metal salts were taken in the round bottom flask. Then to the respective metal salt solution 20 mg drug loaded material was dispersed and allowed to stir for 4 h at room temperature in dark condition. Then filtered very cautiously and filtrate solution was taken for the study of the release of drug molecules. The phosphate buffer was also taken to investigate the release of drug molecules at physiological pH. Here, we prepared 0.1 N $NaH_2PO_4$ and 0.1 N $Na_2HPO_4$ aqueous solutions and physiological pH (*ca.* 7.4) buffer solution was prepared by mixing of the two mixtures with suitable ratio. To 20 mL aqueous buffer solution, 20 mg drug loaded sample was added and allowed to stir for 4 h at room temperature in dark condition. Then

filtered very cautiously and filtrate solution was taken for the study of the release of drug molecules. In both cases the release of drug molecules were investigated by using UV-vis absorption spectroscopy.

***In Vitro* Studies:**

**Cell line and cell culture for determination of non-toxicity and biocompatibility of the encapsulated drug.** Two cancer cell lines, namely, HeLa (human cervical carcinoma) and PC3 (human prostrate adeno carcinoma) cell lines were collected from National Centre for Cell Science, Pune, India. HeLa cells were cultured in DMEM and PC3 cells were grown in RPMI 1640; both the media were supplemented with 10% FBS (Invitrogen Corp.,USA) and 1% antibiotic (Invitrogen Corp., USA) at 37°C in a humidified incubator (Thermo Electron Corporation) with 5% $CO_2$. We performed the cytotoxicity assay first to determine if the antibiotic, or the encapsulated antibiotic was toxic to the cells. We also determined the cytotoxicity, if any, of the chemicals HSMPSNP-1, HSMPSNP-2, used in nano-encapsulation.

**Cytotoxicity Assay.** To test the cytotoxicity, if any, of tetracycline, the encapsulated drug, HSMPSNP-1 and HSMPSNP-2, we did the LDH (lactate dehydrogenase) estimation assay to determine the level of LDH in the cell culture medium. After separate treatment of tetracycline, encapsulated tetracycline, HSMPSNP-1 and HSMPSNP-2 (at 100 µg/ml concentration) for 48 hour, the media were collected from the cell culture petri-dishes where the treatment was initially given and estimation of LDH was done using a commercially available kit (Crest biosystems, India). Values were expressed as mean ± standard deviation. As the assay results showed non-toxicity of each of these treatments, we excluded HSMPSNP-1 and HSMPSNP-2 from further cell viability assay.

**Cell viability Assay.** To test the cytotoxicity of the encapsulated drug (nano-tetracycline) and the antibiotic, tetracycline, MTT assay (that is, 4,5-dimethylthiazol-2-yl-2,S-diphenyltetrazolium bromide assay) was performed according to the procedure described earlier.[1]

After treatment of the encapsulated drug and tetracycline for 48 hour at various concentrations (50, 75, 100, 125 and 175 μg/ml), 10 μL of MTT solution (1 mg/mL in PBS) was poured into each well of a 96-well culture plate containing either HeLa or PC3 cells in media. The culture plates were incubated continuously at 37 °C for 3 hour at dark. Then the media were removed from the wells and replaced with 100 μL of acidic isopropyl alcohol. The intracellular formazan crystals (blue-violet) formed were solubilized with 0.04N acidic isopropyl alcohol, and absorbance of the solution was measured at 595 nm wavelength with a microplate reader. The cell viability was expressed as the optical density ratio of the treatment to control. Values were expressed as mean (%) ± standard deviation. Statistical significance was considered at *$p<0.01$ vs. normal control cells.

**Fluorescence microscopic analysis for biocompatibility assessment.** To examine if the encapsulated drug entered successfully into the cells, we incubated the cells with encapsulated drug at a concentration of 100 μg/ml, for 6 hours HeLa cells (as we could not detect much fluorescence inside the cells at earlier fixation time) and 1 hour for PC3 cells (that showed positive fluorescence), respectively, at 37 °C and photographs were taken under fluorescence microscope. Then a solution of Magnesium chloride (100μg/ml) was added onto the cells, and kept at room temperature for 15 min after which the photographs were taken. This step of adding Magnesium chloride on the cell suspension was repeated thrice at an interval of 15 min, and at each step photographs were taken.

***In Vivo* Studies:**

**Acute toxicity test.** After being sure that the encapsulated tetracycline had no or negligible cytotoxic effects in vitro, we wanted to confirm that this also had no vein clogging effect in vivo. For this, we used Swiss albino mouse (*Mus musculus*) as the mammalian model organism under supervision of the Animal Welfare Committee, Department of Zoology, Kalyani University with Institutional ethical clearance from the University of Kalyani for conducting the *in vivo* experiments. Encapsulated drugs were injected intravenously to the tail veins of the mice (n=3) at concentrations of 1mg, 2 mg and 3 mg, respectively.[2] Experimental animals were observed for next 120 hours (5 days) for any changes in behaviour and mortality. Blood samples collected from the tail veins of the animals (received intravenous injection at 3 mg concentration) were observed under fluorescence microscope at intervals of 1, 2 and 3 hours, respectively.

**Statistical analysis.** Data were analyzed and significance of the differences between the mean values was determined by one-way ANOVA with Dunnett's post-hoc tests, using SPSS 14 software. Statistical significance was considered at $*p < 0.01$.

## ***Section S2: Characterization Techniques:***

**Characterization Techniques.** Powder X-ray diffraction patterns (XRD) of the samples were recorded on a Bruker AXS D-8 Advance diffractometer operated at 40 kV voltage and 40 mA current and calibrated with a standard silicon sample, using Ni-filtered Cu Kα ($\lambda$= 0.15406 nm) radiation. Transmission electron microscopic images were recorded on a JEOL 2010 TEM operated at 200 kV. A Jeol JEM 6700 field emission scanning electron microscope (FE–SEM) with an energy dispersive X-ray spectroscopic (EDS) attachment was used for the determination of morphology of the particles and its surface chemical compositions, respectively. Nitrogen adsorption/desorption isotherms of the samples were recorded on a Quantachrome Autosorb 1C, at 77 K. Prior to the gas adsorption measurements, the samples were degassed at 423 K for 4 h under high vacuum. Fourier transform infrared (FT IR) spectra of these samples were recorded on KBr pellets by using a Nicolet MAGNA-FT IR 750 Spectrometer Series II. UV-visible diffuse reflectance spectra were recorded on a Shimadzu UV 2401PC with an integrating sphere attachment $BaSO_4$ was used as background standard. Thermogravimetric analysis (TGA) and differential thermal analysis (DTA) of the sample were carried out in a TGA instrument thermal analyzer TA-SDT Q-600 under $N_2$ flow. X-Ray photoelectron spectroscopic (XPS) measurements were conducted on the samples using a SPECS (Germany) XPS system with a hemispherical energy analyzer (HSA 3500). A monochromatic Mg $K_\alpha$ X-ray (1253.6 eV) was used as the excitation source operated at 10 kV and with an anode current 17 mA. $^{29}Si$ and $^{31}P$ solid state magic angle spinning nuclear magnetic resonance (MAS NMR) experiments were carried out to evaluate the different chemical environment of the Si and P atoms in the

mesoporous matrix. Bruker advance 500 spectrometer was used here for NMR data recording. Tetramethylsilane (TMS) and phosphoric acid were used as reference for chemical shift measurement for $^{29}Si$ and $^{31}P$, respectively.

For measuring the ion-exchange efficiency of the hollow sphere mesoporous phosphosilicate nanoparticles (HSMPSNPs), 0.100 g of the powder sample was dispersed in 80 mL (0.01M) KCl aqueous solution and the mixture was stirred for 4 h at ambient temperature. Then the dispersed solution was filtered very cautiously. Here, aqueous (0.01M) $AgNO_3$ solution was used to determine the $Cl^-$ concentration in the initial KCl solution and in filtrate solution through titration by using 5 wt% potassium chromate aqueous solutions as indicator. Hence, the exchanged $Cl^-$ concentration and the anion exchange capacity were measured by subtracting the $Cl^-$ ion concentration in the filtrate from the initial KCl solution.

## ***Section S3: Powder XRD:***

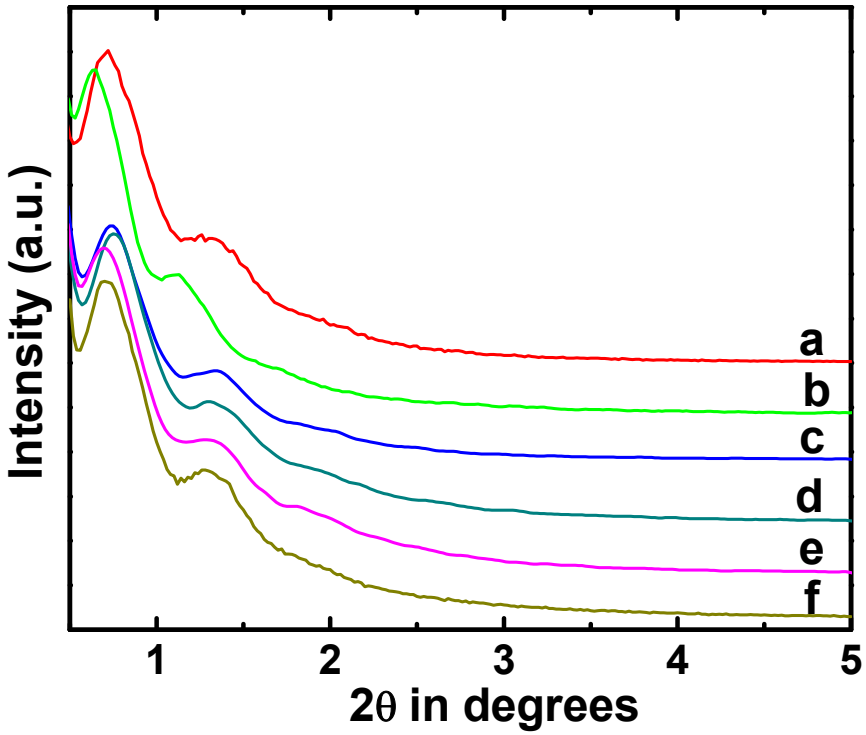


**Fig. S1** Small–angle powder XRD pattern of calcined HSMPSNPs-1 (a), extracted HSMSPSNPs-1 (b), calcined HSMPSNPs-2 (c), calcined HSMPSNPs-4 (d) calcined HSMPSNPs-10 (e) and calcined HSMPSNPs-1 after loading of drug (f).

## ***Section S4: FE-SEM image analysis:***

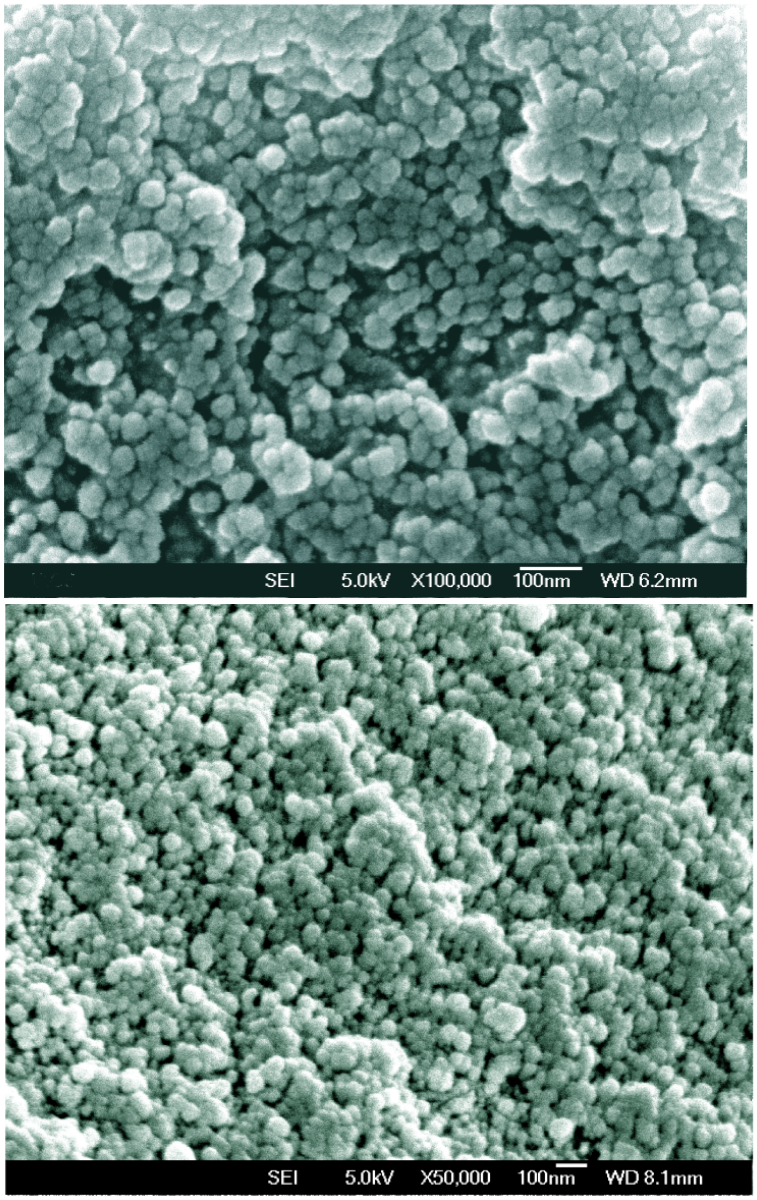


**Fig.S2** FE SEM images of calcined HSMPSNPs-1 (a) and HSMPSNPs-2 (b).

## ***Section S5: Nitrogen Sorption Analysis:***

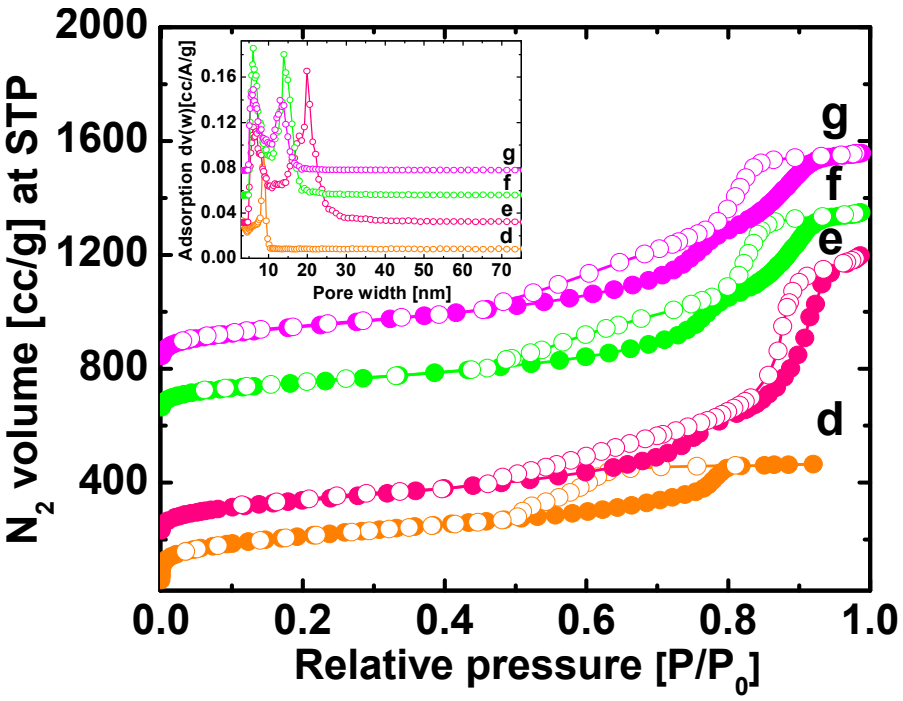


**Fig. S3:** $N_2$ adsorption/desorption isotherms of calcined SBA-15 (d), extracted HSMPSNPs-1 (e), HSMPSNPs-4 (f) and HSMPSNPs-10 (g) measured at 77 K. Y axis of plot d, e, f and g have been enhanced by 100, 250, 630 and 800, respectively for clarity. Adsorption points are marked by filled circles and desorption points by empty circles. Respective pore size distributions using NLDFT method are shown in inset.

**Table S1.** Physico–Chemical Properties of Hollow Sphere Mesoporous Phosphosilicate Nanoparticles (HSMPSNPs).

| Entry | Sample name | Si/P molar ratio | Surface area ($m^2g^{-1}$) | Pore width (nm) | Pore volume ($ccg^{-1}$) |
|---|---|---|---|---|---|
| 1 | HSMPSNPs-1 (calcined) | 1 | 482 | 9.04/22.03 | 1.45 |
| 2 | HSMPSNPs-1 (drug loaded) | 1 | 387 | 5.85/14.97 | 1.30 |
| 3 | HSMPSNPs-2 | 2 | 616 | 6.18/16.06/20 | 1.38 |
| 4 | SBA-15 | - | 611 | 8.7 | 0.64 |
| 5 | HSMPSNPs-1 (extracted) | 1 | 439 | 6.87/19.98 | 1.46 |
| 6 | HSMPSNPs-4 | 4 | 434 | 5.94/13.6 | 1.08 |
| 7 | HSMPSNPs-10 | 10 | 529 | 5.77/13.4 | 1.14 |

## ***Section S6: Infrared Spectroscopy:***

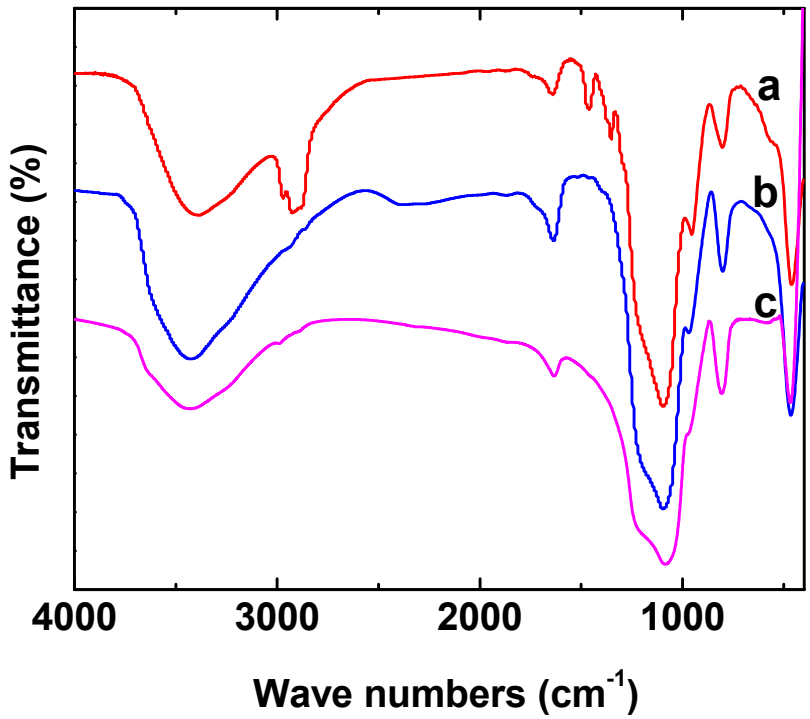


**Fig. S4:** FT IR spectra of (a) as-synthesized HSMPSNPs-1 and (b) calcined HSMPSNPs-1 (c) after drug loading of HSMPSNPs-1 materials.

FT IR spectra of the hollow sphere mesoporous phosphosilicate nanoparticles (HSMPSNPs) are shown in Fig. S4. The FT IR spectra of the HSMPSNPs show the broad envelope in the 1000-1300 $cm^{-1}$ region, where some of the vibration modes overlap the ones typical siloxane as well as the stretching modes of the phosphate network.[3-4] The absorption bands at 800 $cm^{-1}$ (P-O-P and Si-O-Si symmetric stretching),[5] 970 $cm^{-1}$ (stretching of Si-OH bonds),[3] and 1650 $cm^{-1}$ (deformation modes of O-H bonds and of molecularly adsorbed water within the materials)[6] are

also observed. Moreover, all samples exhibit a broad absorption band in the 3000-3750 $cm^{-1}$ range (stretching of O-H bonds)[6-7] These features are clearly displayed in Fig. S4. The shoulder at 3650 $cm^{-1}$ is related to free Si-OH groups,[6,8] while the broad absorption band arises from SiO-H and PO-H group stretches involved in hydrogen bonding. Hydrogen bonding causes low-frequency shifts, the magnitude of which are related to the strength of hydrogen bonds in which the OH groups are involved.[4,6] The peaks at 550 and 970 $cm^{-1}$ almost disappear, indicating that dehydroxylation reactions occur which progressively transform the silica and phosphorous precursors into the phosphosilicate framework.[9]

## ***Section S7: X-Ray Photoelectron Spectroscopy:***

**X-Ray Photoelectron Spectroscopy (XPS).** X-Ray photoelectron spectroscopic studies are carried out for hollow sphere mesoporous phosphosilicate nanoparticles (HSMPSNPs) in order to detect the presence of the different elements as well as their oxidation state in the frameworks. Chemical analysis revealed Si/P and O/(Si+P) molar ratios of 1.23 and 4.83, respectively. Very high O content could be attributed to the high concentration of surface defect sites. Fig.S5 showed the XPS spectra of Si 2p and P 2p. In Fig.S5A a broad single peak is observed with binding energy of 104.07 eV, due to the Si 2p which confirms the presence of silica in $Si^{4+}$ oxidation state with four oxygen neighbors in the HSMPSNPs.[10-11] Absence of any peak near 99.0 eV implies that no silica in $Si^{0}$ oxidation state is present in the HSMPSNPs.[12] The peak at 135.22 eV for P 2p can be considered as evidence for the pentavalent state of phosphorous present within this material as shown in the Fig.S5B.[13] Furthermore, a single broad peak is observed at 533.35 eV, could be attributed to the O 1s spectrum as shown in Fig.S6.[14]

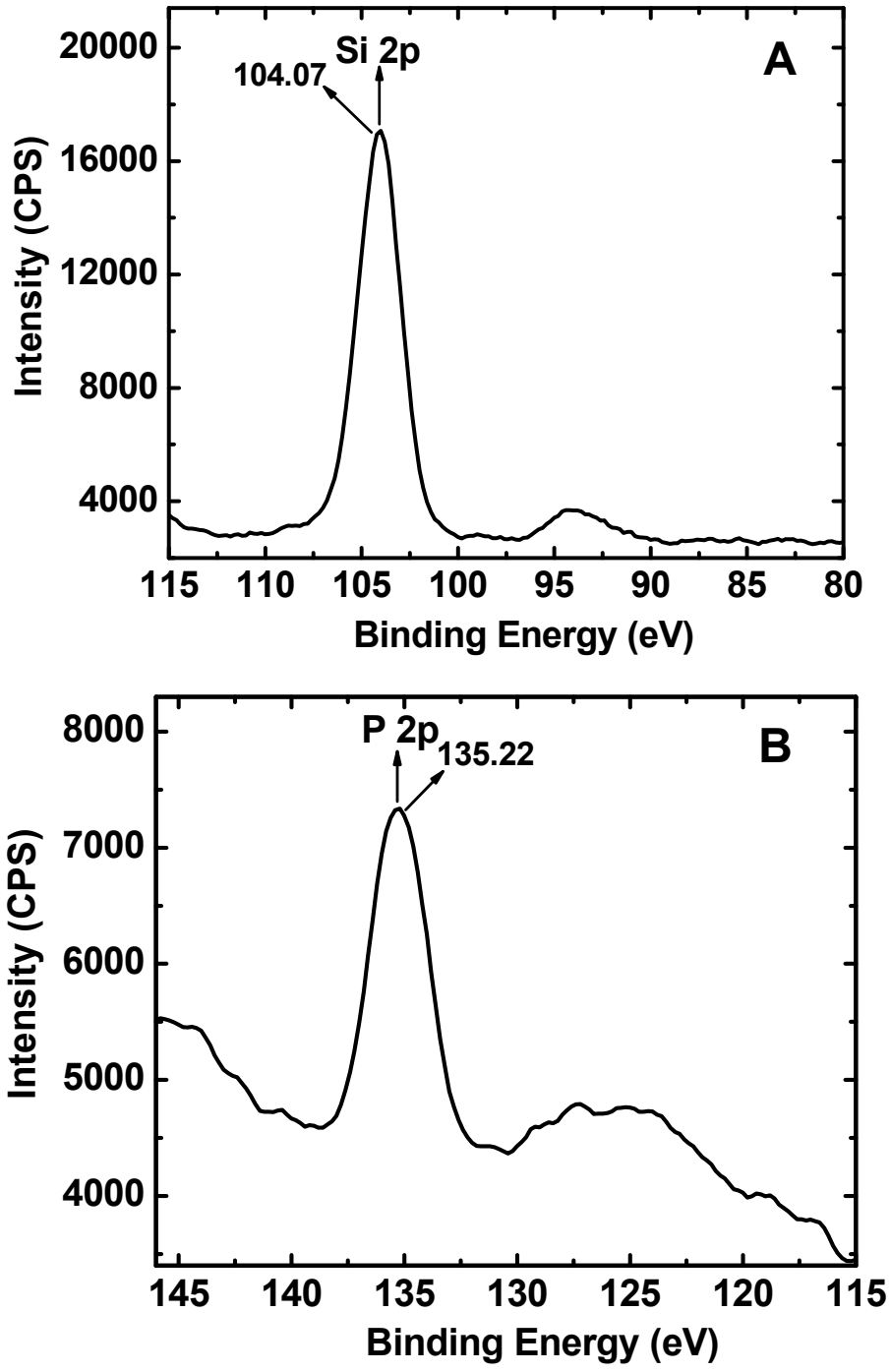


**Fig. S5:** XPS of Si 2p (**A**) and P 2p (**B**) for HSMPSNPs-1.

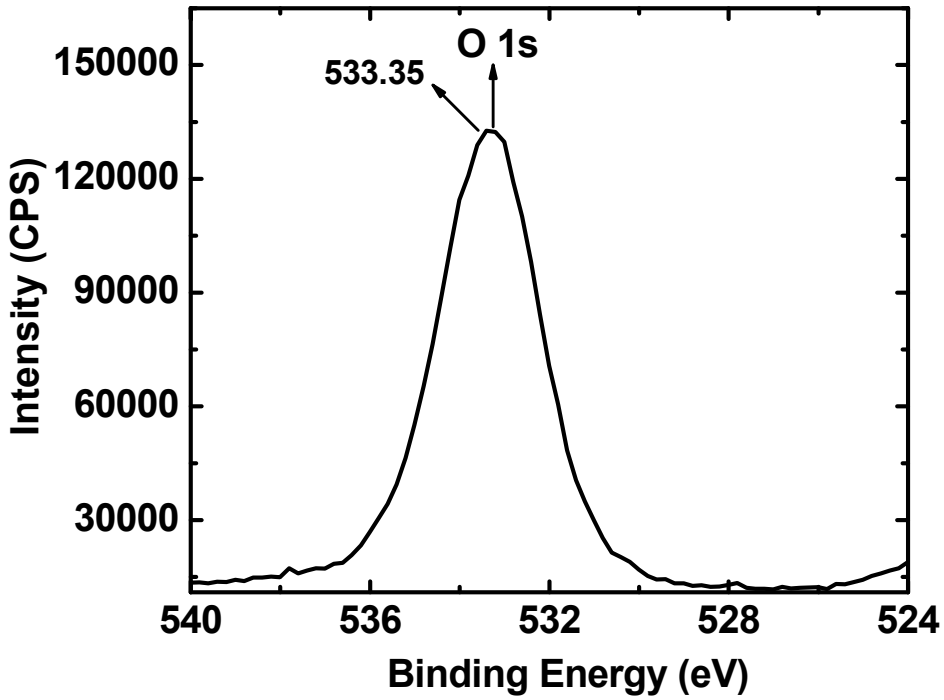


**Fig.S6:** XPS of O 1s for HSMPSNPs-1.

## ***Section S8: Solid state MAS NMR Spectroscopy:***

**$^{29}$Si and $^{31}$P Solid State MAS NMR Study.** For further investigating the chemical environment of the silicate frameworks, $^{29}$Si solid state MAS NMR spectra of the HSMPSNPs-1 sample has been taken which is shown in Fig.S7a. $^{29}$Si NMR (Fig. S7a) of HSMPSNPs material exhibits two peaks at *ca.* -110 and *ca.* -100 ppm that can be assigned to $Si(OSi)_4$ ($Q^4$) or $Si(OSi)_2$-(OP)(OH) and $Si(OSi)_3(OH)$ ($Q^3$) or Si(OSi)(OP)$(OH)_2$ chemical environments, respectively. Considerable downfield chemical shifts for all these peaks maxima in comparison with pure mesoporous silica SBA-15 suggest the phosphorous incorporation adjacent to the $SiO_4$ tetrahedral units.[15-16] The presence of phosphorous atoms in the vicinity of $SiO_4$ tetrahedral unit may also generate Si(3Si, P) and Si(2Si, 2P) like local chemical environments which could significantly contribute to the large downfield chemical shifts.

Moreover, to determine the chemical environment of the phosphorous in the HSMPSNPs-1 material, we have also performed $^{31}$P solid state MAS NMR spectra as shown in Fig.S7b. This material exhibits three signals (Fig.S7b) at -9 ($q^1$), -15 ($q^2$) and -32 ppm ($q^3$), due to the presence of O=P(OSi or OP) $(OH)_2$, O=P(OSi or OP)$_2$ (OH), and O=P$(OP)_m(OSi)_n$, (where, m + n = 3) environments, respectively.[17-18] Furthermore, a broad intense signal in the $^{31}$P NMR spectra is observed at *ca*. 0 ppm ($q^0$) which is due to $H_3PO_4$. Thus, the $^{29}$Si and $^{31}$P solid state MAS NMR studies thus reveal the presence of tetrahedral Si and P species. Thus the $PO_4$ and $SiO_4$ tetrahedras would be cross-linked to form covalent networks in the HSMPSNPs.

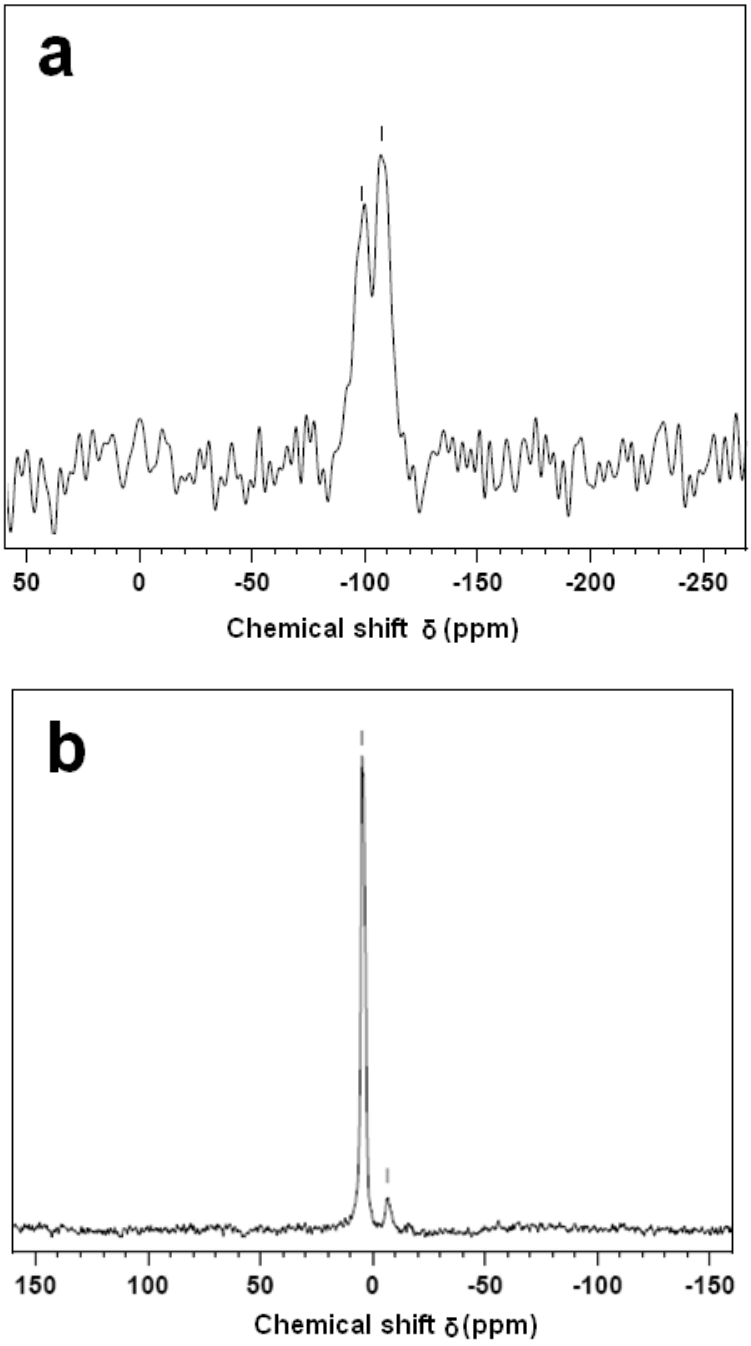


**Fig.S7:** $^{29}$Si solid state MAS NMR (a) and $^{31}$P solid state MAS NMR (b) spectra of HSMPSNPs-1.

## ***Section S9: Framework Structure:***

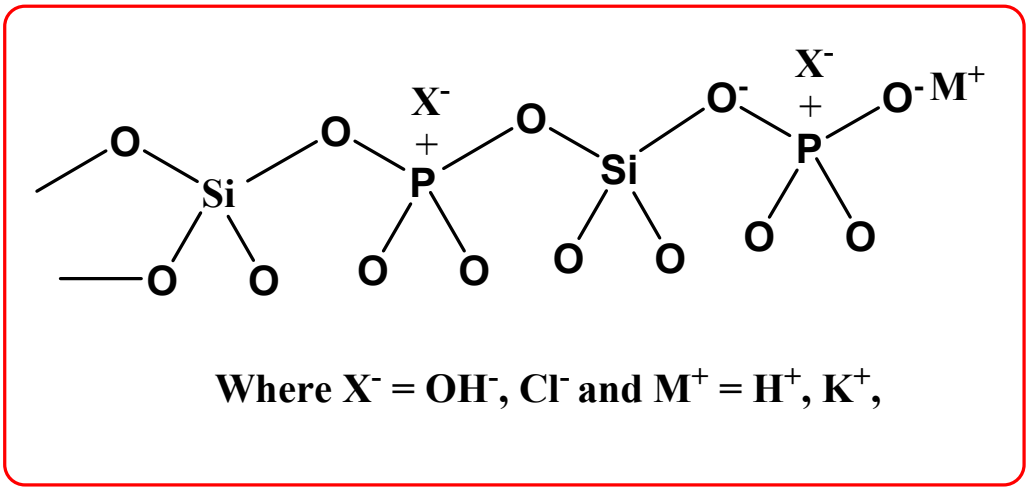


**Fig. S8:** Proposed framework structure of HSMPSNPs.

## ***Section S10: Structure of Tetracyclin Drug:***

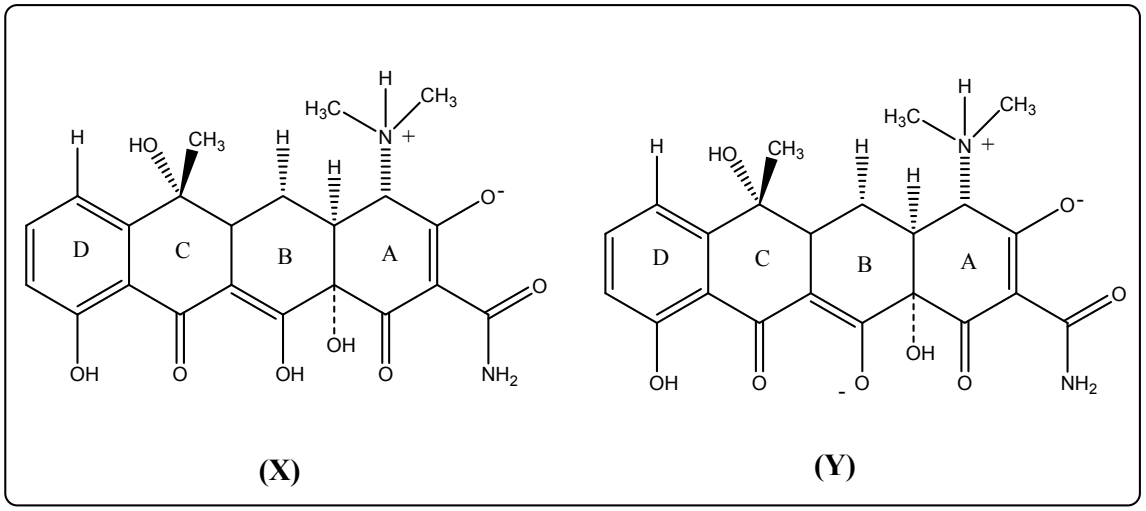


**Fig. S9:** Structure of tetracycline: (X) zwitterions tetracycline species (84%) and (Y) anion tetracycline species (16%).

## ***Section S11:*** *Solid state UV–vis diffuse reflectance Spectroscopy:*

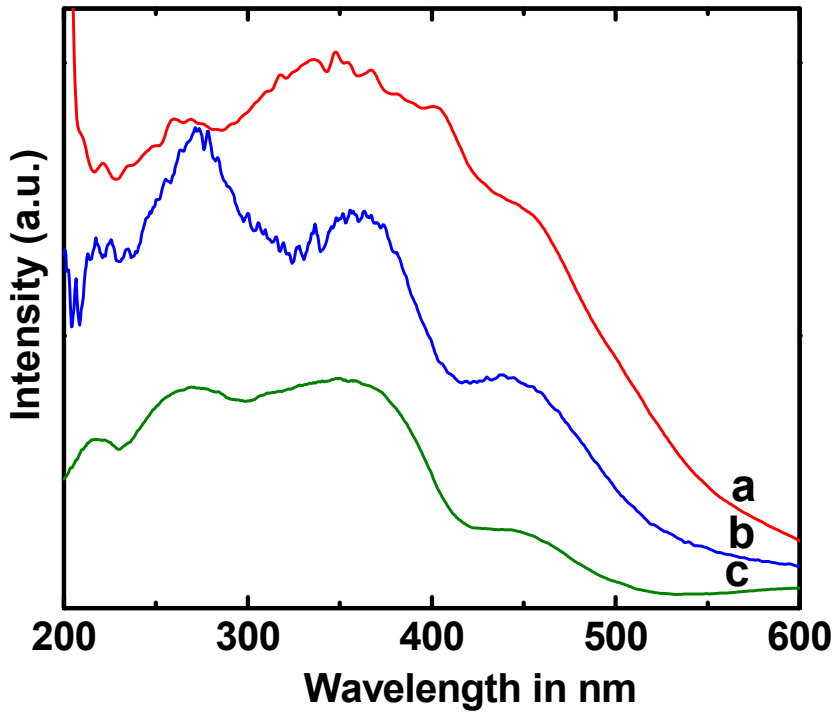


**Fig. S10:** UV–vis diffuse reflectance spectrum of pure tetracycline (a) drug (tetracycline) loaded HSMPSNPs-1 (b) and drug (tetracycline) loaded HSMPSNPs-2 (c).

## ***Section S12: Solution state UV–vis absorption Spectroscopy:***

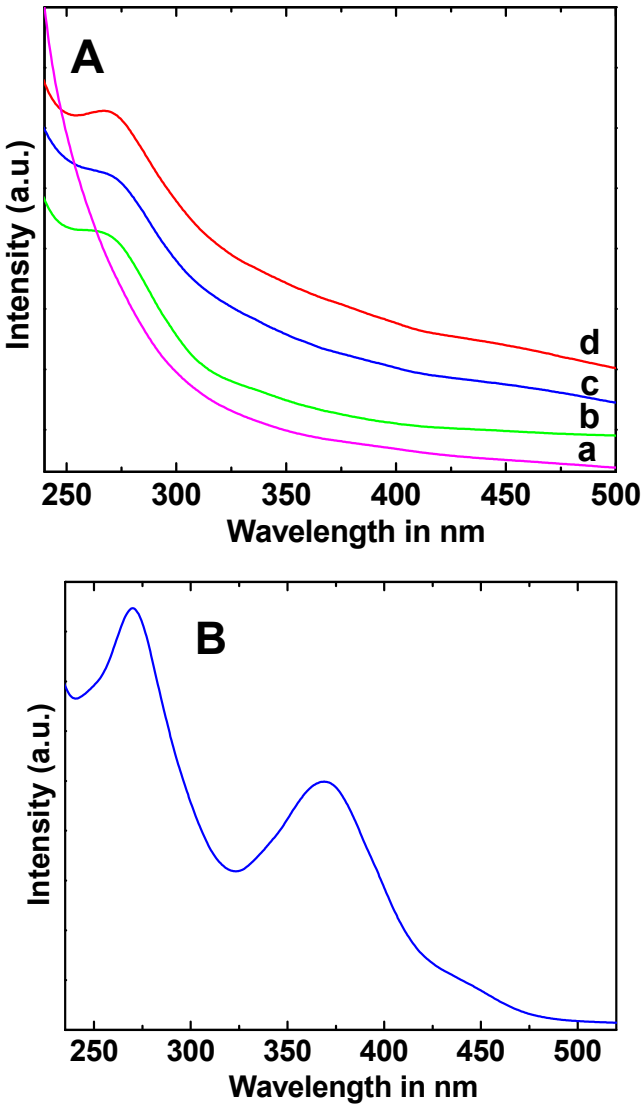


**Fig. S11: A**: UV–vis absorption spectrum of the filtrate solution after treatment with (a) $Cu^{2+}$ (a), $Ca^{2+}$ (b), $Zn^{2+}$ (c), and $Mg^{2+}$ (d) cations with drug loaded HSMPSNPs-1. **B**: UV–vis absorption spectrum of the filtrate solution after treatment with phosphate buffer solution at physiological pH (ca. 7.4) with drug loaded HSMPSNPs-1.

## ***Section S13: Cell Studies:***

**Cell Studies**. Analysis of data of LDH assay revealed that there was no significant change in LDH level in different experimental groups after 48 hour of incubation at a concentration of 100µg/ml (Fig. S12), the dose which was further used in fluorescence microscopic studies.

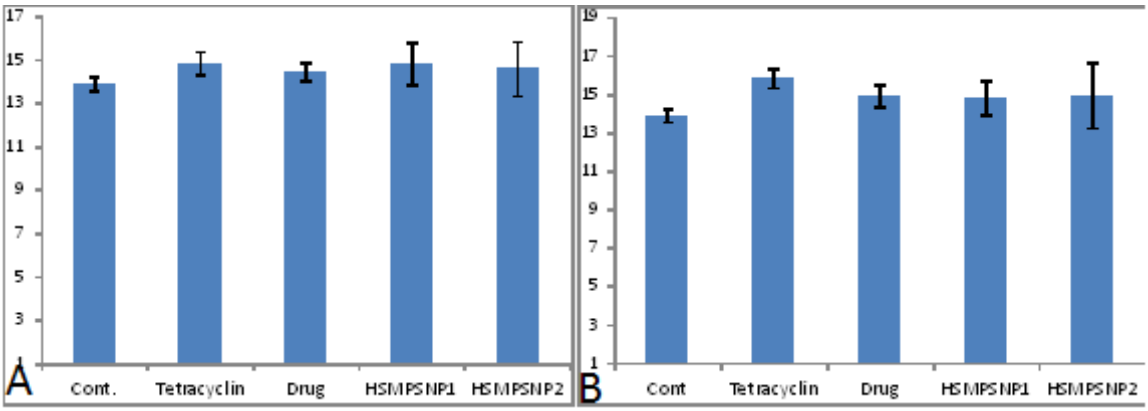


**Fig. S12:** (Cytotoxicity assay): Histogram represents the cytotoxicity of tetracycline, encapsulated drug, HSMPSNP-1 and HSMPSNP-2 at 100 µg/ml concentrations on HeLa (A) and PC3 (B) cells, after 48 hours of incubation.

Results of MTT assay at various concentrations of the encapsulated drug for up to 48 hour have been shown in Fig. S13. No significant cell death occurred even at 48 hour incubation of the encapsulated drug at concentration up to 150 µg/ml drug. This would therefore suggest that the encapsulated drug can be readily used for cellular application at the indicated dose and time of incubation without worry about its cytotoxicity.

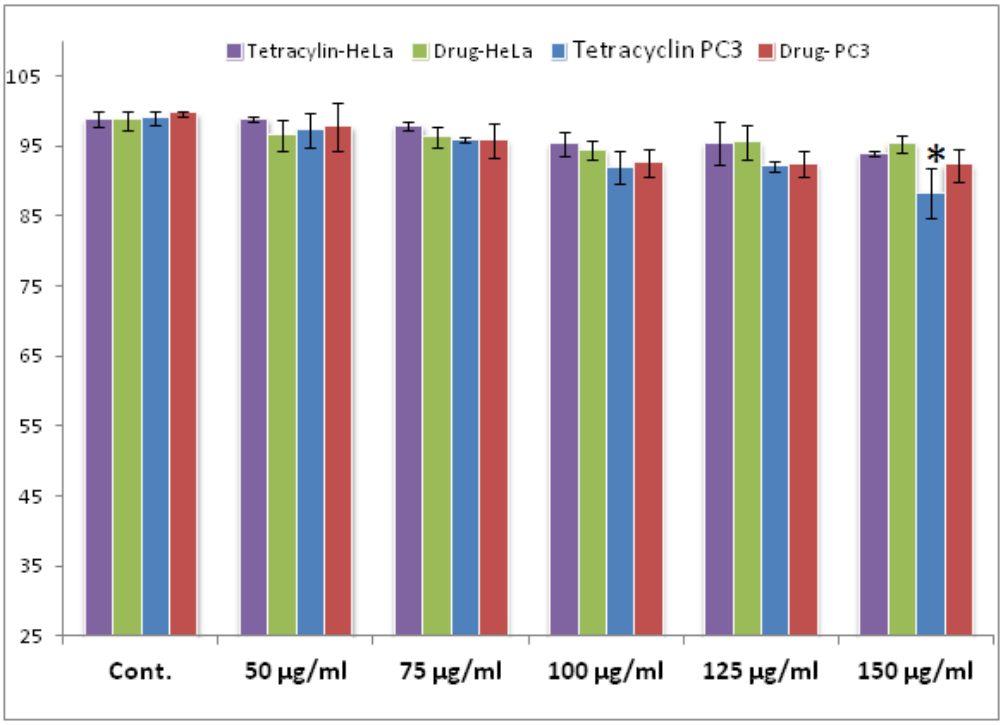


**Fig. S13:** (Cell viability assay): Histogram represents the cytotoxicity of the encapsulated drug and tetracycline at various concentrations on HeLa and PC3 cells, after 48 hours of incubation.

The intracellular fluorescence behavior of the drug was studied on both HeLa and PC3 cells at several fixation time points. After incubation with the encapsulated drug at 37 °C for the earlier mentioned time points (6 hr for HeLA cells and 1 hr for PC3 cells), the cells displayed a gradual increase in intra-cellular fluorescence in HeLa cells from 15 min onward when Magnesium chloride was added in the medium, but in PC3 cells there was an almost similar degree of fluorescence right from 15 min through 45 min (Fig. S14). Apparently, the fluorescence behavior inside cells of PC3 was more pronounced than in HeLa cells, indicating thereby that cells of different tissue origin may have differential response to the deposition of the encapsulated drug inside cell.

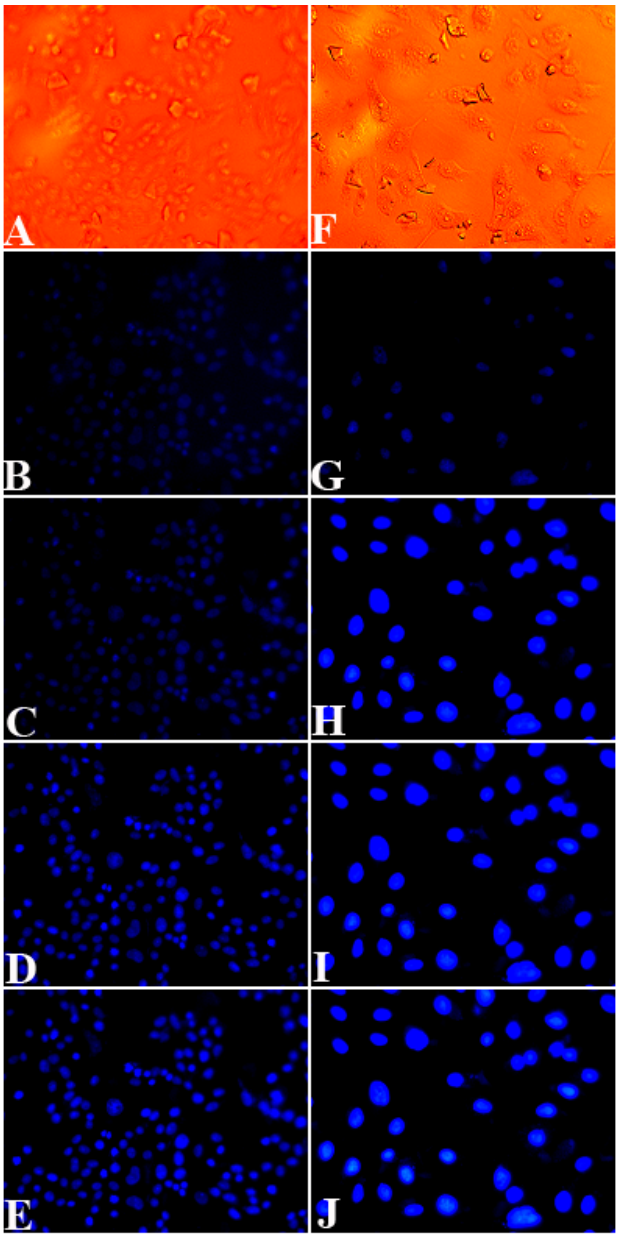


**Fig. S14:** (Fluorescence microscopic observations): (A) Phase contrast image of HeLa cells and (B) fluorescence image of HeLa cells incubated with 100 µg/ml encapsulated drug for 6 hours at 37 °C. Cells were exposed to added extracellular Magnesium chloride (C-E). (F) Phase contrast image of PC3 cells and (G) fluorescence image of PC3 cells incubated with 100 µg/ml encapsulated drug for 1 hour at 37 °C. Cells were exposed to added extracellular Magnesium chloride (H-J).

## ***Section S14: In Vivo Studies:***

**Effect on encapsulated drug on survivability and blood flow.** We observed that there was no apparent abnormality of blood cells or blockage of veins (resulting in cardiac arrest) or any other toxic behaviour of the encapsulated drug on the blood cells of experimental mice. Mice injected with the encapsulated drug behaved quite normally during the 120 hours (5 days) without a single mortality or change in feeding behaviour for all the doses tested. Fluorescence microscopic observations of blood from experimental animals revealed that fluorescence of the encapsulated drug persisted in blood for about an hour, after which it disappeared rapidly, and then totally disappeared at 4 h (Fig. S15). This would indicate that the drug did not clog the veins, but was possibly deposited or absorbed into some other tissue.

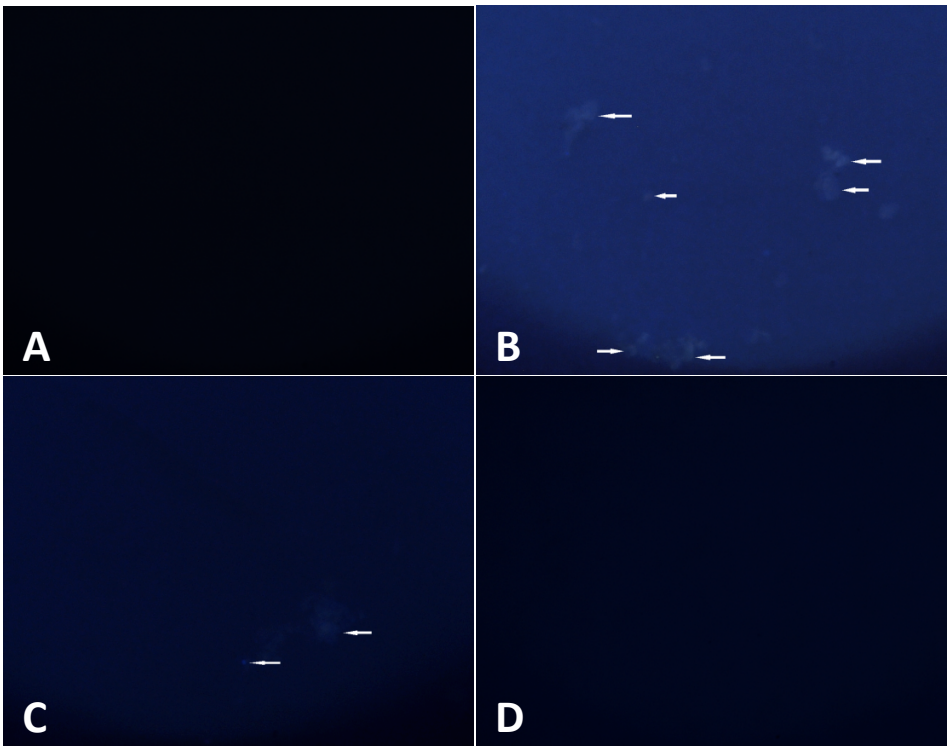


**Fig. S15:** (Fluorescence imaging of blood sample of mice): Fluorescence image of blood samples of mice; A: normal mouse without any drug treatment (control), B: 1 hour after drug treatment, C: 2 hours after drug treatment, D: 4 hours after drug treatment.

## References

1 J. Ratha, K. A. Majumdar, S. K. Mandal, R. Bera, C. Sarkar, B. Saha, C. Mandal, K. D. Saha and R. Bhadra, *Mol. Cell. Biochem*. 2006, **290**, 113.

2 L. Shapira, W. A. Soskolne, Y. Houri, V. Barak, A. Halabi and A. Stabholz, *Infection And Immunity*, Mar. 1996, 825–828.

3 J. Gallardo, A. Dura´n, D. Di Martino and R. M. Almeida, *J. Non-Cryst. Solids,* 2002, **298**, 219-225.

4 O. Pawlig and R. Trettin, *Chem. Mater.,* 2000, **12**, 1279-1287.

5 P. Innocenzi, *J. Non-Cryst. Solids,* 2003, **316**, 309-319.

6 M. Cerruti, G. Magnacca, V. Bolis and C. Morterra, *J. Mater. Chem.,* 2003, **13**, 1279-1286.

7 M. D'Apuzzo, A. Aronne, S. Esposito, P. Pernice, *J. Sol-Gel Sci. Technol.,* 2000, **17**, 247-254.

8 J. D. Sunseri, W. T. Cooper and J. G. Dorsey, *J. Chromatogr. A,* 2003, **1011**, 23-29.

9 A. Aronne, M. Turco, G. Bagnasco, P. Pernice, M. D. Serio, N. J. Clayden, E. Marenna and E. Fanelli, *Chem. Mater.,* 2005, **17**, 2081-2090.

10 K. McEleney, C. M. Crudden and J. H. Horton, *J. Phys. Chem. C,* 2009, **113***,* 1901-1907.

11 J.A. Navío, M. Macías, G. Colón, P.J. Sánchez-Soto, V. Augugliaro and L. Palmisano,

*Appl. Surf. Sci.,* 1994, **81**, 325-329.

12 F. Rochet, G. Dufour, H. Roulet, B. Pelloie, J. perriere, E. Fogarassy and A. M. Slaoui Froment, *Phys. Rev. B* **1988**, *37,* 6468-6477.

13 G.D. Khattak, A. Mekki and L.E. Wenger, *J. Non-Cryst. Solids,* 2009, **355**, 2148-2155.

14 S. K. Das, M. K. Bhunia, M. M. Seikh S. Dutta and A. Bhaumik, *Dalton Trans.,* 2011, **40**, 2932-2939.

15 M. Paul, N. Pal, M. Ali and A. Bhaumik, *J. Mol. Catal. A: Chem.,* 2010, **330**, 49-55.

16 D. Epping and B. F. Chmelka, *Curr. Opin. Colloid Interface Sci.,* 2006, **11**, 81-117.

17 O. Neeraj, M. Eswaramoorthy and C. N. R. Rao, *Mater. Res. Bull.,* 1998, **33**, 1549-1554.

18 A. García, M. Colilla, I. Izquierdo-Barba and M.Vallet-Regí, *Chem. Mater.,* 2009, **21**, 4135–4145.